



OPEN ACCESS

EDITED BY Luca Brocca, National Research Council (CNR), Italy

REVIEWED BY
Sabri Kanzari,
National Research Institute for Rural
Engineering, Water and Forestry (INRGREF),
Tunisia
Zhenyu Zhang,
University of Illinois at Urbana-Champaign,
United States

*CORRESPONDENCE Eshrat Fatima ☑ eshrat.fatima@ufz.de Rohini Kumar ☑ rohini.kumar@ufz.de Martin Schrön ☑ martin.schroen@ufz.de

RECEIVED 16 May 2025 ACCEPTED 15 September 2025 PUBLISHED 03 November 2025

CITATION

Fatima E, Kumar R, Altdorff D, Attinger S, Boeing F, Oswald SE, Rakovec O, Samaniego L, Zacharias S and Schrön M (2025) On the value of mobile cosmic-ray neutron measurements for spatio-temporal soil moisture simulations. *Front. Water* 7:1630051. doi: 10.3389/frwa.2025.1630051

COPYRIGHT

© 2025 Fatima, Kumar, Altdorff, Attinger, Boeing, Oswald, Rakovec, Samaniego, Zacharias and Schrön. This is an open-access article distributed under the terms of the Creative Commons Attribution License (CC BY). The use, distribution or reproduction in other forums is permitted, provided the original author(s) and the copyright owner(s) are credited and that the original publication in this journal is cited, in accordance with accepted academic practice. No use, distribution or reproduction is permitted which does not comply with these terms.

On the value of mobile cosmic-ray neutron measurements for spatio-temporal soil moisture simulations

Eshrat Fatima^{1,2*}, Rohini Kumar^{1*}, Daniel Altdorff^{1,2}, Sabine Attinger^{1,2}, Friedrich Boeing^{1,2}, Sascha E. Oswald², Oldrich Rakovec³, Luis Samaniego^{1,2}, Steffen Zacharias⁴ and Martin Schrön^{4*}

¹Department of Computational Hydrosystems, UFZ-Helmholtz Centre for Environmental Research GmbH, Leipzig, Germany, ²Institute of Environmental Science and Geography, University of Potsdam, Potsdam, Germany, ³Faculty of Environmental Sciences, Czech University of Life Sciences Prague, Prague, Czechia, ⁴Department of Monitoring and Exploration Technologies, UFZ-Helmholtz Centre for Environmental Research GmbH, Leipzig, Germany

High-resolution soil moisture measurements are indispensable for advancing hydrological modeling and improving environmental risk assessments at regional scales. However, it remains an open question to what level hydrological models are capable of representing spatio-temporal patterns of root-zone soil moisture. In this study, we present a novel integration of mobile Cosmic-Ray Neutron Sensor (CRNS) data collected via rail-based measurements into the mesoscale Hydrologic Model (mHM). Over ten months, daily CRNS observations had been acquired along a 9-km railway corridor and subsequently aggregated to a \sim 200 m, spatial resolution to align with the mHM resolution. Soil moisture related model parameters were optimized for distinct land cover types based on observed soil moisture dynamics, including dense forest, open forest, meadow, and railway shunting areas. Model simulations exhibited considerable improvements with Nash-Sutcliffe Efficiency (NSE) values increasing from -0.19 to 0.76 in the dense forest, and from 0.50 to 0.79 in the meadow with homogeneous land cover conditions. In contrast, areas characterized by mixed land use-such as half-open forests and railway yards exhibited lower performance, indicating areas of improvements in the model-data fusion scheme including higher resolution that may be necessary to fully capture local variability. Further, results of the spatio-temporal analysis demonstrated the model ability to reproduce observed spatial patterns of CRNS derived soil moisture with the spatial efficiency (SPAEF) score of 0.71 (1.0 being an ideal one). Finally, the transferability of the optimized parameters was evaluated by applying them to independent sites located 38-345 km away from the original measurement corridor. The reasonably good agreement between simulated and observed soil moisture at grassland sites further confirms the robustness and applicability of our model-data fusion approach, while substantial biases remain in forest sites. Overall, the integration of mobile CRNS measurements represents a new era for hydrological modeling by providing unprecedented

spatial resolution and temporal coverage to facilitate more precise soil moisture estimations for effective water resource management, and forecasting of floods and droughts.

KEYWORDS

soil moisture, cosmic-ray neutron measurements, MHM, model-data fusion, spatio-temporal analysis, parameter transferability

1 Introduction

Soil moisture (SM) plays a critical role in the terrestrial water cycle, influencing key processes such as evapotranspiration, infiltration, and runoff. Accurate knowledge of SM dynamics is essential for applications ranging from weather forecasting to flood and drought risk assessment, irrigation planning, and climate change impact studies (Seneviratne et al., 2010; Samaniego et al., 2013; Corradini, 2014; Samaniego, 2025). However, existing methods for measuring the SM have limitations on accuracy and resolution. In situ sensors offer high temporal but limited spatial resolution, while satellite-based sensors (e.g., SMOS, SMAP) provide broader coverage (~ 10 km resolution) but are restricted to shallow depths (0-5 cm) and are influenced by surface and atmospheric conditions such as cloud vegetation (Fang et al., 2024; Entekhabi et al., 2014). These limitations underscore the need for more representative ground-based SM observations at the horizontal and vertical scales to improve the reliability of the hydrological model (Oswald et al., 2024).

To overcome the limitations of conventional soil moisture observation techniques, recent advances have focused on the use of cosmic ray neutron sensing (CRNS), which provides spatially integrated soil moisture measurements on intermediate scales, typically up to 10-20 hectares, with an effective sensing depth of up to 80 cm (Zreda et al., 2008; Schrön et al., 2018a; Köhli et al., 2021; Bogena et al., 2022). Unlike point-scale sensors, CRNS captures a representative average on a footprint, reducing the spatial mismatch often encountered when integrating observations with hydrological models (Andreasen et al., 2017; Baatz et al., 2017; Zheng et al., 2024; Fatima et al., 2024; Scheiffele et al., 2025; Arnault et al., 2025). However, most CRNS installations have been stationary, offering limited spatial coverage and often failing to capture fine-scale heterogeneity across landscapes. Recent advances in mobile and rail-based CRNS platforms mark a significant step forward in large-scale soil moisture monitoring. These systems enable continuous large-scale soil moisture monitoring along railways, providing high spatial and temporal resolution of soil moisture at medium scales across diverse landscapes (Schrön et al., 2021; Altdorff et al., 2023). This mobile CRNS capability fills a critical gap between traditional in-situ monitoring and coarseresolution satellite observations.

Hydrological models simulate the terrestrial water cycle and predict soil moisture (and other state variables) in unobserved locations or future states, relying on observational data for calibration and validation (Fatichi et al., 2016; Gnann et al., 2023). However, these models are highly dependent on observational data, which are often scarce, leading to significant uncertainties in the model predictions (Renard et al., 2010; Teweldebrhan et al., 2018; Moges et al., 2020).

Several studies have demonstrated the use of CRNS data to parametrize hydrological and land surface models at intermediate soil depths (Han et al., 2015; Baatz et al., 2017; Iwema et al., 2017; Duygu and Akyürek, 2019; Patil et al., 2021; Fatima et al., 2024; Arnault et al., 2025). These studies underscore CRNS's ability to capture soil moisture dynamics at relevant spatial scales, offering a significant advantage over traditional point-scale measurements for model calibration. The simulation of CRNS-derived soil moisture in hydrological models has led to an improved representation of soil moisture dynamics, particularly within the root zone (Fatima et al., 2024). Notable benefits include enhanced estimates of water balance components, more accurate evapotranspiration modeling, and better parameter transferability across heterogeneous landscapes.

However, these studies have also made it clear that there are still major gaps in the provision of representative data of the temporal dynamics of soil moisture at model-relevant scales. It is evident that conventional stationary sensors, including stationary CRNS probes, are incapable of addressing this discrepancy. The recent advancements in mobile CRNS technology have enabled the acquisition of high-resolution data on soil moisture dynamics on a larger scale, both temporally and spatially. Still, the processing of such data gives rise to new challenges, particularly with regard to the interpretation of the CRNS signal under varying vegetation cover, soil texture, and atmospheric conditions, highlighting the need for robust correction and calibration techniques. The present study addresses these challenges and tests for the first time the integration of a continuous time series of rail-based CRNS data.

The framework integrated into the mesoscale hydraulic model (mHM; Samaniego et al., 2010b), which enables the simulation of neutron counts to assess soil moisture accuracy, was demonstrated by Fatima et al. (2024). In the present study, the integration of rail-based Cosmic-Ray Neutron Sensor (CRNS) data offers an opportunity to expand this approach to larger spatial scales. This work aims to evaluate the capability of the data-model fusion scheme integrating the mobile CRNS measurements into mHM for simulations of root-zone soil moisture (RZSM) patterns at regional scales across various land use types. We also assess the generality of such a data-model fusion scheme by cross-validating the model parameterizations established using the railway CRNS data at remote stationary CRNS sites. This is done to evaluate the modeling potential to improve soil moisture representation at ungauged sites.

In this paper, we investigate the use of observational data from a fully automated rail-based CRNS system for soil moisture simulations in a large-scale mHM model. The measurement data provide continuous soil moisture (or soil water content: SWC) on a \sim 9 km railway segment between Blankenburg-Rübeland, Germany (Altdorff et al., 2023). This approach offers novel insights

into the spatio-temporal variations of the SWC in diverse land covers, such as grasslands, dense forests, and open forests. The objectives of this study are 1) to demonstrate the value of high-resolution CRNS measurements for regional scale soil moisture predictions by their integration into a large-scale hydrological model (mHM), and (2) to evaluate the effectiveness of site-specific constrained model parameterizations, based on rail-based CRNS data, for soil moisture simulations at other (ungauged) locations via cross-validation experiments.

2 Data and methods

2.1 Study area

We make use of rail-based CRNS data published by Altdorff et al. (2023) along a \sim 9 km long railway segment between Blankenburg-Rübeland, Germany (Figure 1). Observational railbased CRNS data were collected using a novel mobile CRNS system installed in the locomotive of a cargo train designed for continuous automated CRNS measurements. This system covers a segment of the railway and provides hectare-scale neutron counts, revealing spatial soil moisture patterns on a medium scale. The datasets were recorded from September 2021 to July 2022. The elevation of the area ranges from 217 to 482 meters (asl). The experimental railway track crosses four different types of land cover: dense and open forest, semi-natural areas, and meadows. The main texture of the soil is silty loam soil, which has been extensively studied by Yang et al. (2018); Winter et al. (2021). During the period 1999 to 2019, Blankenburg recorded an average annual temperature of °C and an average annual precipitation of 760 mm (Altdorff et al., 2023). For a more detailed analysis of the climatic characteristics of the Rübeland region, (see Wollschläger et al., 2017). Furthermore, the red pins on the German map mark the locations of the crossvalidation sites: Grosses Bruch, Hohes Holz, Kall, Rollesbroich, and Wildenrath. These sites, which have been extensively discussed in Bogena et al. (2022), Li et al. (2024), Baatz et al. (2017), Baatz et al. (2014), and Bogena et al. (2018), are utilized here for crossvalidation purposes.

2.2 The mesoscale hydrological model (mHM)

In our study, we used the mHM (Samaniego et al., 2010b; Kumar et al., 2013b), https://www.ufz.de/mhm, which is a distributed hydrologic model that integrates the main hydrological processes: snow accumulation and melting, evapotranspiration, canopy interception, soil water infiltration, percolation, and runoff generation. Inputs to the model consist of meteorological datasets (i.e., daily precipitation, potential evapotranspiration, and average air temperature), morphological datasets (i.e., digital elevation model, slope, aspect, flow direction, and flow accumulation), and soil/hydrogeological properties (i.e., layer-wise soil characteristics, such as bulk density, sand, and clay content).

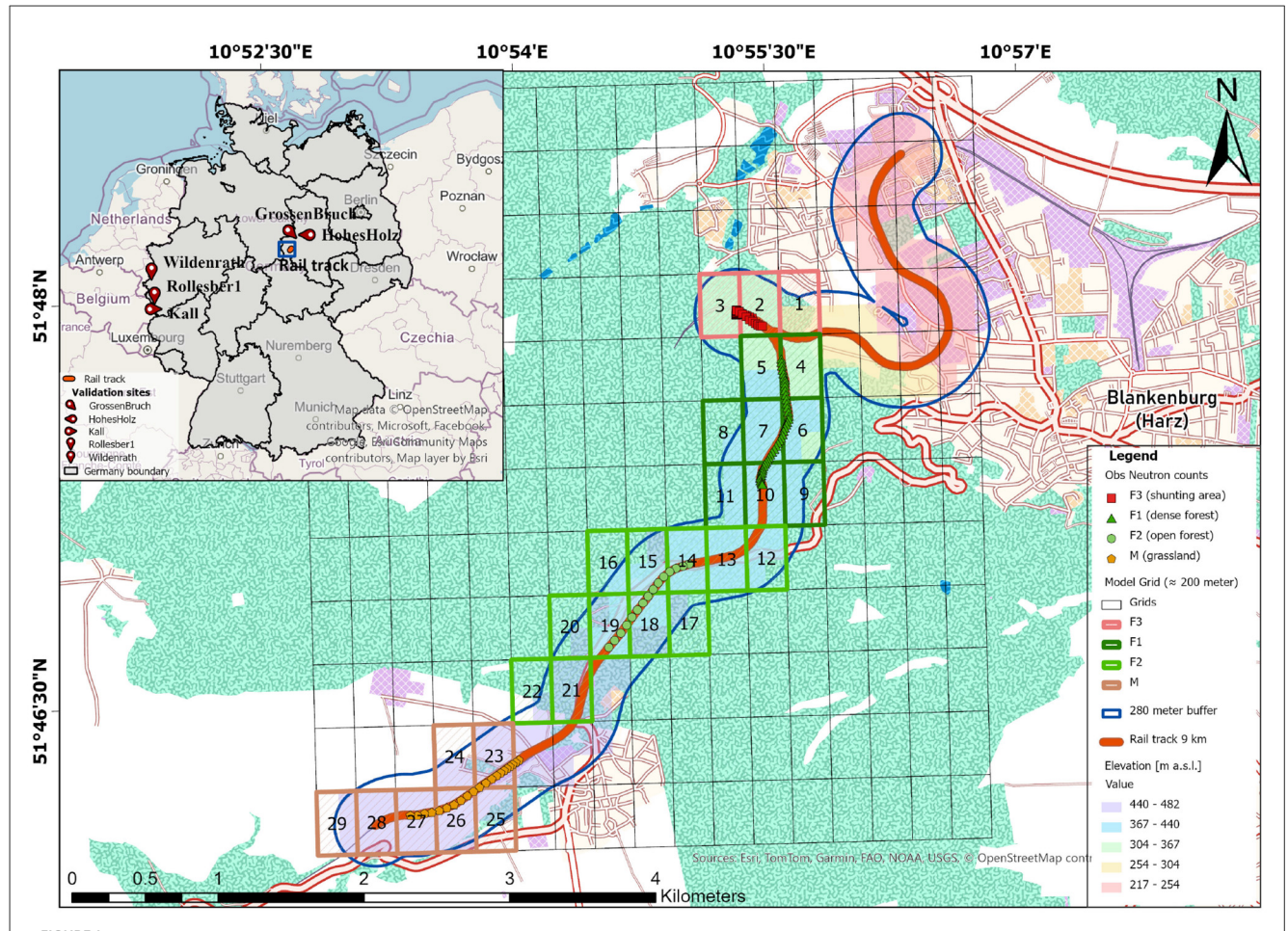
mHM is structured into three spatial levels: Level 0 (ℓ_0) focuses on gathering detailed physical characteristics of the land under study, Level 1 (ℓ_1) integrates these characteristics to simulate

hydrological processes, and Level 2 (ℓ_2) applies meteorological data to drive these simulations accurately. mHM uses a unique feature, multiscale parameter regionalization, (MPR; Samaniego et al., 2010b; Kumar et al., 2013b) to estimate effective hydrologic model parameters. This approach effectively utilities fine-scale (ℓ_0) spatial variability in terrain and landscape attributes, including soil and vegetation types to parameterize hydrologic model parameters. MPR relies on the idea of estimating model parameters (e.g., soil porosity) based on physiographical properties (e.g., sand and clay content) and transfer functions (e.g., pedotransfer functions) at a fine scale, at which physiographical attributes are available (ℓ_0) . Transfer functions include functional relationships and global parameters (e.g., factors of the pedotransfer functions) which are generally inferred via calibration (Samaniego et al., 2010b; Kumar et al., 2013b). In the subsequent step of MPR, the ℓ_0 derived model hydrologic parameters are aggregated to the modeling scale (ℓ_1) using upscaling operators (e.g., arithmetic or harmonic means).

Further details on mHM code can be found at https://mhmufz.org and underlying modeling concepts at Samaniego et al. (2010a) and Kumar et al. (2013b). An overview of the global parameters and the resulting effective model parameters can be found in Supplementary Table S1. The SM dynamics in mHM are modeled using the infiltration capacity (IC) approach, which simulates vertical fluxes by allowing water movement in a oneway downward direction. The mHM model, utilizing this ICbased soil moisture distribution scheme, has demonstrated strong performance in predicting fluxes and state variables (e.g., Rakovec et al., 2016; Boeing et al., 2022) and is effective in generating transferable parameters (e.g., Kumar et al., 2013a; Samaniego et al., 2017). The saturated SM content θ_s (m³ m⁻³) is calculated using pedo-transfer functions (PTFs) from Zacharias and Wessolek (2007). The land use data in mHM are divided into three broad categories: coniferous and mixed forest (class 1); impervious areas like settlements, highways, and industrial parks (class 2); and pervious areas covering fallow lands, agricultural fields, and pastures (class 3). For the present study, the soil horizon was divided into three layers with the following depths: shallow layers (0-5 cm and 5-25 cm) and a deep layer (25-60 cm); and an average depth of (0-60 cm) was used additionally for comparison. An overview of the datasets used in the model is provided in Table 1.

2.3 Neutron counts modeling

Since CRNS measures the area-average neutron density rather than soil moisture directly, it differs from traditional point-based soil moisture measurements. The technique provides spatially integrated observations on a larger area (150–200 m radius), which makes CRNS suitable for evaluating distributed hydrological models like mHM. The effective integral measurement depth varies as a function of the soil moisture between $\sim 15~\rm cm$ for moist soils and 80 cm for dry soils (Köhli et al., 2015). Thus, the exact contribution of each soil layer depends on the vertical distribution of moisture, which changes over time. As a result, it is difficult to directly match CRNS-derived soil moisture values with specific layers in the model. To avoid this mismatch, we simulate neutron counts directly inside mHM based on the soil moisture profile,



Geospatial distribution of observed neutron counts and mHM resolution within the study site, highlighting the four different land cover areas: F3 (grids 1–3; shunting area), F1 (grids 4–11; dense forest), F2 (grids 12–22; open forest), and M (grids 23–29; meadow). [@ OpenStreetMap contributors 2021; distributed under the Open Data Commons Open Database License (ODbL) v1.0].

TABLE 1 Overview of the input data used in mHM, including their spatial resolutions and data sources.

Variables	Products	Spatial resolution	Temporal resolutionReferences	
Level 2: meteorological data				
Precipitation	DWD	~0.2 km (0.00390625°)	Daily	Kaspar et al. (2013); Zink et al. (2017); Boeing et al. (2022) [Link]
Temperature (avg, min, and max)	DWD	~0.2 km (0.00390625°)	Daily	Kaspar et al. (2013); Zink et al. (2017); Boeing et al. (2022) [Link]
Level 0 & 1: morphological data		(0.001953°)		
Terrain characteristics (elevation, slope, aspect, flow direction, and flow accumulation)	GMTED 2010	225 m (0.0021°)	Static	USGS (2017) [Link]
Soil properties (horizon depth, bulk density, sand and clay content)	BUEK200	250 m (0.0023°)	Static	BGR (2020) [Link]
Geology	GLiM v1.0	0.5°	static	Hartmann and Moosdorf (2012) [Link]
Land use/land cover	Globcover	300 m (0.0028°)	Static	ESA and UCLouvain (2010) [Link]
Phenology (leaf area index)	GLCF	8 km (0.0833°)	Bimonthly	[Link]
Model calibration/evaluation In-situ	data			
Rail-based CRNS	NCs/SM data	~ 30 m	Daily	Altdorff et al. (2023) [Link]

DWD, German Weather Service; GLCF, Global Land Cover Facility; GLiM, Global Lithological Map; GMTED, Global Multi-resolution Terrain Elevation Data; BUEK, Bodenübersichtskarte; NCs, Neutron counts.

which ensures a consistent comparison between model outputs and CRNS observations. This neutron model implements the vertically weighted Desilets method across various land cover types as described in detail by Fatima et al. (2024).

The simulations are performed at a spatial resolution of 200 m \times 200 m, allowing the representation of spatial variability in soil moisture and land surface characteristics. The model was calibrated using rail-based CRNS measurements collected along a railway segment (see details in Section 2). Calibration involved directly comparing observed and simulated neutron counts, with model performance assessed by maximizing the Nash-Sutcliffe Efficiency (NSE) (Nash and Sutcliffe, 1970). This method uses a weighted SWC ($\theta_{\rm avg}$) approach by Schrön et al. (2017) at soil horizon depths of 0–5 cm, 5–25 cm, and 25–60 cm, along with other fitting parameters, i.e., $a_0=0.0808$, $a_1=0.372$, $a_2=0.115$, and $N_{0,{\rm Des}}=22888$ cph. The $N_{0,{\rm Des}}$ is fixed for the railway sensor system determined by Altdorff et al. (2023) on the basis of field measurements. It is the count rate on dry soil under the same reference conditions.

$$N_{\text{Des}} = N_{0,\text{Des}} \left(\frac{a_0}{\left(\theta_{\text{avg}} + \theta_{\text{lw}}\right) / \varrho_b + a_2} + a_1 \right). \tag{1}$$

For lattice water, we assume a linear relationship to clay content (Avery et al., 2016):

$$\theta_{\text{lw}} = \theta_{\text{lw}0} \cdot C + \theta_{\text{lw}1} \,, \tag{2}$$

where C denotes the clay fraction in % Greacen (1981). The quantity of derived lattice water, $\theta_{\rm lw}$, is regionalized based on C and varies between 0.0 and 0.1 m³ m⁻³.

Figure 2 presents the flow diagram of our study; we used mHM to simulate SWC in various types of land cover. The model requires multiple input datasets, including meteorological data (precipitation and temperature), morphological datasets (elevation, geology, and land cover), and soil datasets (BUEK200); the data source is given in Table 1. These datasets serve as primary inputs to define the hydrological conditions in the study area. The model parameters focus on key hydrological variables, specifically snow, soil moisture, and neutron count dynamics, which are essential to simulate water balance dynamics. For the comparison of soil moisture patterns from CRNS and mHM, we use the gravimetric soil moisture product from CRNS, and convert the modeled SWC to gravimetric soil moisture using $\theta_{\rm grv} = {\rm SWC}/\varrho_{\rm b}$, where $\varrho_{\rm b}$ is the dry soil bulk density.

2.4 Calibration and evaluation

A large number of combinations of randomly generated model parameters are needed to quantify the uncertainties of the model parameters and their influence on the model results. An established sampling method is the Monte Carlo method, while a more efficient method is Latin hypercube sampling (LHS), as derived from the work of McKay and Conover (1979). This method improves the representativeness of the sample space by dividing the range of each variable into equal probability intervals and randomly selecting

a value from each interval, thus maintaining the randomness of sample selection.

Latin hypercube sampling was performed, with 10^5 runs varying 27 global model parameters in mHM. Details of parameter selection can be found in Supplementary Table S1. The time from 2017 to 2022 was selected as the simulation period, while only the last year was used for the analysis to minimize the influence of the initial conditions. Calibration was performed using field data from four distinct sites representing different land cover conditions: (*F1* – *F3* and *M*).

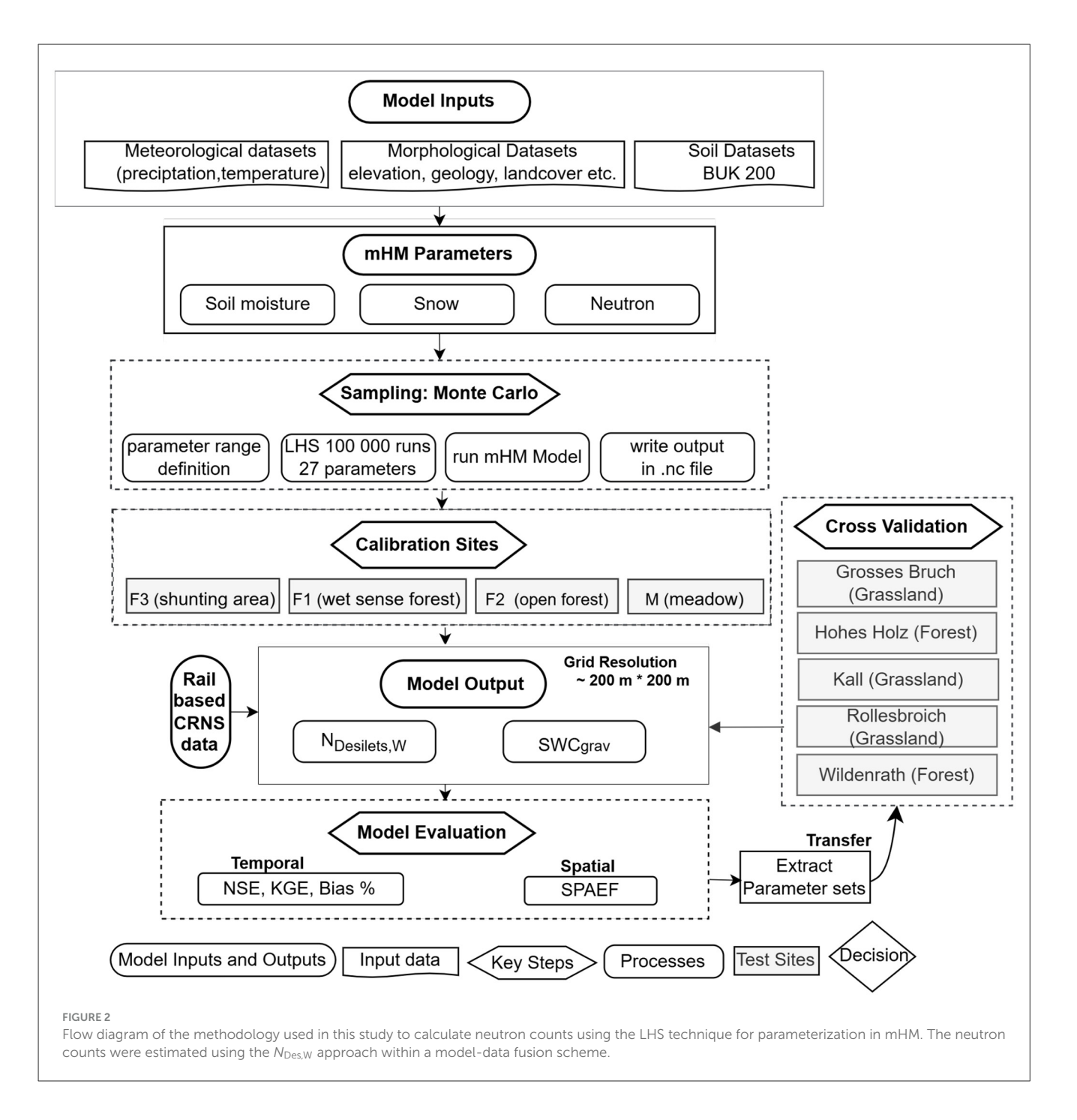
To compare the simulated neutron counts with the observed rail-based CRNS data, the observed data with 30 meter resolution were upscaled to the model grid resolution of $\sim 200~\text{m}$ (i.e., the Level-0 of mHM) using the Inverse Distance Weighting (IDW) approach as described by Shepard (1968). This ensured that the observed data were comparable to the simulated neutron counts with the same spatial scale. The comparison was performed for the period from September 2021 to July 2022.

To assess mHM temporal performance, we used four performance metrics: Nash-Sutcliffe Efficiency (NSE) (Nash and Sutcliffe, 1970), Kling-Gupta Efficiency (KGE) (Gupta et al., 2009), percent bias (PBIAS) (Moriasi et al., 2007), while spatial accuracy was evaluated using the spatial efficiency (SPAEF) metric (Demirel et al., 2018; Koch et al., 2018; Demirel, 2020). The SPAEF metric calculates the spatial pattern similarity between observed and simulated variables using three equally weighted components: correlation (*A*), variability (*B*), and histogram match (*C*). It is mathematically expressed as

SPAEF =
$$1 - \sqrt{(A-1)^2 + (B-1)^2 + (C-1)^2}$$
, (3)

where A is the Pearson's correlation coefficient, B is the ratio of coefficients of variation, and C is the histogram intersection percentage. SPAEF version 2.0 auto-detects the number of bins for histogram calculation, ensuring optimal comparison of spatial patterns. A SPAEF value closer to 1 indicates excellent agreement, while a value closer to 0 suggests poor performance. The SPAEF formulation is inspired by KGE, which is characterized by equally weighted components of variability, correlation, and bias. Previously, SPAEF was applied successfully to model studies on evapotranspiration (Demirel et al., 2018), soil moisture (Eini et al., 2023), snow water equivalent (SWE) (Tiwari et al., 2023), actual evapotranspiration (ET_a) (Demirci and Demirel, 2023; Soltani et al., 2021; Nguyen et al., 2022), and satellite-derived land surface temperature (Duethmann et al., 2024).

We preferred NSE as an objective function to constrain the model parameters based on neutron counts measurements because it evaluates how well the model captures the variability in the observed data, rather than just matching the mean or total volume. A cross-validation experiment was performed using independent data sets from five test sites to further demonstrate the generality and/or transferability of the presented modeling scheme: *Grosses Bruch* (grassland), *Hohes Holz* (forest), *Kall* (grassland), *Rollesbroich* (grassland), and *Wildenrath* (forest). The calibrated parameter sets from the primary study sites (railway segment between Blankenburg-Rübeland) of the site *F1* and *M* were transferred and applied to these test locations to assess model transferability. This was done by extracting the 10 optimized

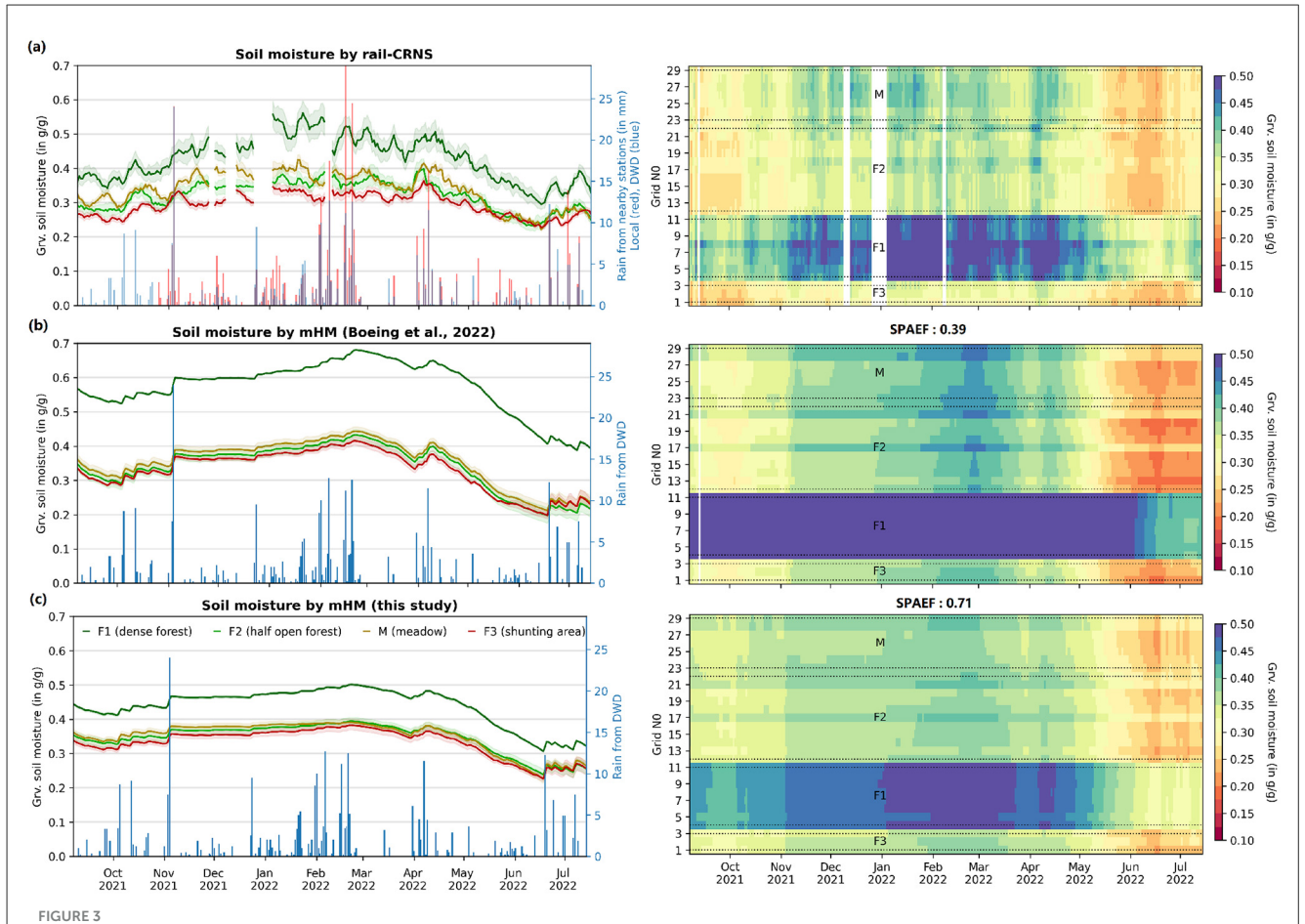


parameter sets and making decisions on model reliability based on cross-validation results. To further evaluate our results, we utilized the mHM simulations established by Boeing et al. (2022) as a default (reference) mHM simulation. We initially tested the mHM parameters using the GDM setup by Boeing et al. (2022), which were calibrated against streamflow using a multi-basin approach optimized with KGE and the DDS algorithm across 201 catchments. Notably the German drought monitor (GDM) setup https://www.ufz.de/index.php?en=37937 uses Boeing et al. (2022) as a reference and this will allow us to quantify the improvements achieved in our approach relative to those employed by the GDM.

3 Results and discussion

3.1 Comparison of soil moisture patterns from rail-based CRNS and mHM simulations

The Figure 3 presents a comparative analysis of rail-based CRNS measurement data with the mesoscale hydrological model (mHM) to improve soil moisture simulations in different types of land cover. The left panels (a-c) illustrate the temporal dynamics of the mean values for sites *F3* (grids 1–3), *F1* (grids 4–11), *F2* (grids 12–22), and *M* (grids 23–29),



Comparison of soil moisture estimates from different methods across various land cover types. (a) Soil moisture measurement using rail-based cosmic-ray neutron sensing (rail-CRNS). (b) Soil moisture was simulated using mHM from Boeing et al. (2022) used in the GDM. (c) Soil moisture was simulated using mHM in this study. The left panels show a time series of soil moisture (g/g) for different land cover types (F1 - dense forest, F2 - half-open forest, F3 - shunting area, M - meadow), along with precipitation data. The right panels display the spatial distribution of soil moisture over time from Oct 2021 to July 2022 for different grid locations.

while the right panels represent their spatial patterns in all grids.

For our analysis, we selected 29 grid cells of mHM at a resolution of 200 m \times 200 m: 3 grid cells for F3, 8 for F1, 11 for F2, and 7 for M. The measurement uncertainty is indicated in panel a) and ranges from $0.02 \, \text{g/g}$ in the meadow to $0.05 \, \text{g/g}$ in the forest based on the estimations provided by Altdorff et al. (2023).

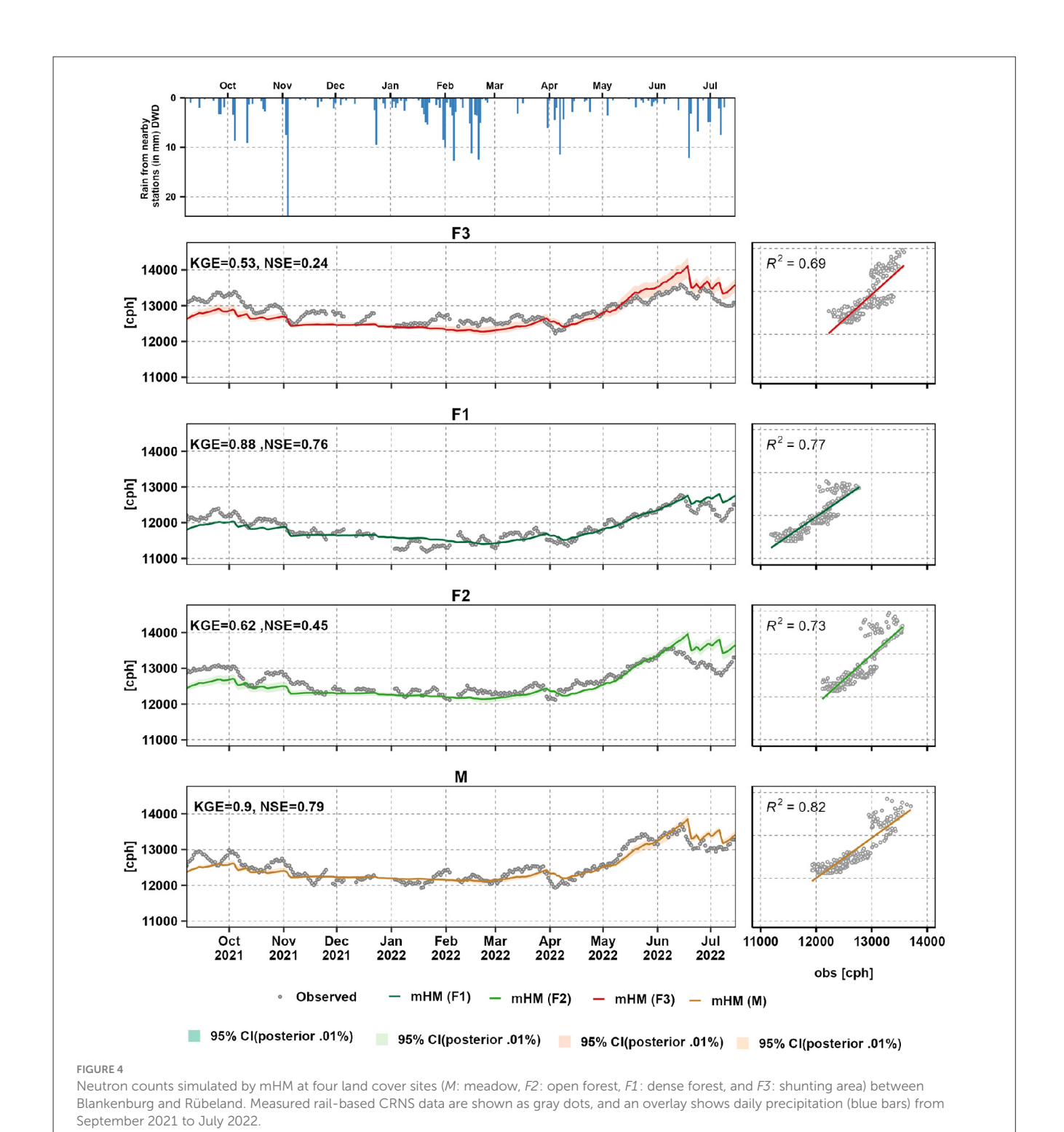
We initially tested the mHM parameters of the German Drought Monitor (GDM) setup by Boeing et al. (2022) by applying them to the railway segment between Blankenburg-Rübeland. Comparison with observations highlighted the need for site-specific calibration, particularly at site F1, where the model overestimates soil moisture. The simulated value remains consistently above 0.5 g/g, resulting in a uniform blue color in the heatmap that indicates unrealistically wet conditions. To address this, we performed a regional calibration of the mHM parameters for these sites. Panel (b) presents the results using the parameters from Boeing et al. (2022), which yielded a SPAEF score of 0.39, a histogram match of 0.77, a correlation coefficient (CORR) of 0.9, and a coefficient of variation (CV) of 1.55.

In panel (c), the soil moisture simulated by the site-specific calibrated mHM of our study shows closer alignment with the CRNS observations compared to the field observations in panel (a). This agreement is particularly strong in dense forests F1 and meadows M. This indicates that the calibration data effectively constrains mHM parameters for the specific region, leading to better performance. However, discrepancies remain, particularly in areas with mixed land cover, such as the half-open forest (F2), and the shunting area (F3), where the model struggles to capture small-scale heterogeneity that exists within an mHM grid point. The shunting area at F3 (i.e., a railway yard and an industrial site) consistently showed the driest conditions in the measurement. This is characterized by a relatively open forest structure with two to three parallel railway tracks, which probably contributes to its persistently drier environment than other forested areas. Surfaces, such as the heterogeneous mix of soil, roads, and buildings in urban areas, can also affect the CRNS signal (Schrön et al., 2018b). However, the mHM model was unable to capture these local features.

Winter bias is likely due to uncertainties in the simulation of frozen soils and snow cover (Thober et al., 2015). Including

meteorological drivers in snow-dominated regions, the choice of the model is the main source of uncertainty (Marx et al., 2018). In addition, the mHM lacks a full energy balance model, which limits its ability to represent soil frost depths. In comparison, the calibrated parameter sets achieved a significantly higher SPAEF score of 0.71, along with improved metrics: a histogram match of 0.77, a CORR of 0.90, and a CV of 0.85 shown in the Supplementary Figure S1. The higher SPAEF score (0.71) and

CORR (0.90) for the calibrated parameters suggest that the mHM model effectively represents the spatial distribution of neutron counts along the railway track. However, some discrepancies remain, which was likely due to the model's limited ability to fully capture vegetation dynamics and fine-scale heterogeneity in land cover. The optimal parameter sets derived from the railway segment between Blankenburg and Rübeland were then cross-validated at uncalibrated sites to assess the performance of the



mobile CRNS data and determine whether sufficient information was available to transfer these parameters. The results can be found in Section 3.4).

3.2 Calibration of mHM to daily rail-based CRNS data

Figure 4 presents a comparison of daily neutron counts from rail-based CRNS measurements and mHM simulations over four types of land cover over a 10-month period. The corresponding performance metrics are summarized in Table 2 and Supplementary Figure S4. Since CRNS observations provide an integral value for soil moisture with varying depth and higher sensitivity to shallow soil horizons, the data cannot be directly compared with modeled SWC from discrete layers. Instead, we simulated the CRNS neutron signal inside mHM based on the physical principles of this depth-sensitivity and compared this value with the measurement neutrons (Fatima et al., 2024). Using the match between observed and modeled neutrons in an objective function, the calibrated model parameters will indirectly result in improved SWC representations for all soil layers. We selected three layers for the soil horizons: 0-5 cm, 5-25 cm, and 25-60 cm. The choice of layering in this study was also made by modeling choices (0-5 cm layer as litter layer, 25-60 cm layer to read out agricultural relevant soil depth).

The objective functions of NSE were used to quantify the degree of matching of the simulated neutron counts with the measured rail-based neutron counts. From the 10⁵ parameter sets, the 10 optimal parameter sets were selected, and their mean was calculated. The results (Figure 4) show that at sites F1 and M, the model demonstrates robust performance with an NSE of 0.76-0.79. In contrast, sites F2 and F3 show discrepancies between observed and simulated data, with NSE values of 0.24 and 0.45, indicating a weaker performance. At both F1 and M sites, the simulation and measurements align closely for most months. However, during the summer months (June to September), we observe a noticeable mismatch between the simulated and measured neutron counts, which is in the order of the average variation of neutron measurements along this track (Altdorff et al., 2023). Specifically, the model tends to overestimate in June and July while underestimating in September and October.

In our mHM setup, the land cover was represented using three dominant classes, forest, permeable, and impervious—derived from the (ESA and UCLouvain, 2010) database. We used a spatial resolution of $\sim 200~\text{m} \times 200~\text{m}$ for land cover, which limits the model's ability to resolve subgrid heterogeneity (Zink et al., 2017). As a result, mixed land cover types within a single grid cell—such as areas containing both forest and bare soil—are not explicitly distinguished. However, there are good correlations for F2 and F3, and the r-squared values of 0.73 and 0.70, respectively, indicate a strong linearity between the simulated and observed data. The site *M* shows the highest model precision among the sites, with an NSE of 0.79. The r-squared value of 0.82 implies good predictive capacity and a strong linear correlation with the observed data. During the winter months from November to March, the temporal variability of the simulated neutron counts showed minimal variation near full

TABLE 2 Performance metrics of neutron counts for model calibration from Sep 2021 to Jul 2022 using various methods: Nash-Sutcliffe efficiency (NSE), Kling-Gupta efficiency (KGE), spatial efficiency metric (SPAEF), coefficient of determination (r-squared), and percent bias (PBIAS) across different land cover.

Track section	Land cover	Performance matrix					
		NSE	KGE	r-squared	PBIAS		
F1	Dense forest	0.76	0.88	0.77	-0.1		
F2	Open forest	0.45	0.62	0.73	-0.6		
F3	Shunting area	0.24	0.53	0.70	-0.7		
М	Meadow	0.79	0.90	0.82	-0.3		

soil moisture saturation (Boeing et al., 2022). The overestimation of neutron counts in June and July indicates dryer soil in the model, while other effects from vegetation water could also contribute to this observation (Baatz et al., 2015). Overall, we find that the forest root fraction coefficient, the organic matter content, and the infiltration shape factor are the most sensitive parameters for this study. The temporal dynamics of neutron counts is better represented for meadow sites.

One of the main challenges identified in this study is the resolution mismatch between mHM and observed CRNS data. Although mHM operates at a grid resolution of ~ 200 m that is comparable with the CRNS footprint, the detection mechanism of neutrons is non-linearly sensitive to the near field, e.g., to soil moisture in the nearest ~ 30 m around the rail track (Schrön et al., 2023). This discrepancy affects the performance of the model in heterogeneous landscapes where the land cover changes more granularly around the rail track, so that the single land cover characteristic assigned to the larger model grid loses representativeness.

Another limitation is the absence of vegetation dynamics in the parameterization of the model, which can lead to systematic biases in the model output, especially regarding root water uptake and soil moisture, as highlighted in previous studies (Zink et al., 2017; Massoud et al., 2019). The inclusion of a dynamic LAI could be useful, as it would influence evapotranspiration, infiltration, and plant-soil water exchanges. Recent advances have introduced a Parsimonious Canopy Model (PCM) that simulates the daily dynamics of LAI and gross primary productivity (GPP) based on temperature and photosynthetically active radiation (Bahrami et al., 2022). This model provides a prognostic and process-based representation of LAI, allowing for improved coupling of vegetation and hydrologic processes. Although promising, this canopy model has not yet been integrated into mHM, limiting the ability to fully represent vegetation-soil in our simulations.

Moreover, the study relied on a single year of CRNS data (September 2021 to July 2022), which may not fully capture interannual variability in meteorological conditions. Extending the dataset to multiple years would improve model robustness and generalizability of our findings.

TABLE 3 Performance assessments for the cross-validation experiment regarding the transferability of at-site calibrated parameters to other sites along with the reference run (mHM-default) simulations by Boeing et al. (2022).

Grassland	Grosses Bruch		Kall		Rollesbroich	
	mHM default	М	mHM default	М	mHM default	М
NSE	-1.51	0.5	0.1	0.37	0.45	0.56
KGE	0.53	0.78	0.61	0.61	0.58	0.47
R ²	0.70	0.65	0.53	0.65	0.58	0.66
PBIAS	-44.3%	9.2%	15.2%	12%	7.4%	0.5%
Forest	Hohes Holz		Wildenrath			
	mHM default	F1	mHM default	F1		
NSE	-16.00	-13.61	-5.39	-12.42		
KGE	-0.32	-0.24	0.20	-0.12		
\mathbb{R}^2	0.82	0.84	0.67	0.68		
PBIAS	132%	122.1%	74%	110%		

3.3 Model performance

The analysis aimed to evaluate the performance of the mHM model at different land cover types for representing soil moisture patterns and dynamics using the closely related neutron count rate. The various efficiency metrics are shown in Table 3 and in the Supplementary Figure S3. The 10 optimal parameter set distributions are summarized in Supplementary Figures S4-S7. The coefficient of determination (R²) also supports the finding that the model performs well in the meadow (M) and halfopen forest areas (F2), with CDFs indicating high correlation values close to 1. The KGE and NSE further underpinned these findings, with the meadow (M) and denser forests (F1) achieving high-efficiency scores close to 1, while half-open forests (F2) and shunting areas (F3) display lower scores. The results from the Cumulative Distribution Function (CDF) indicate that land cover has a significant impact on the mHM's ability to simulate neutron counts. The model shows high performance in open and halfopen areas (M and F1). In contrast, the denser forests (F2) and shunting areas (F3) present the lowest performance, potentially due to the heterogeneous nature of these areas that affect soil moisture dynamics, which are not adequately captured by the model.

This suggests a need for the model to incorporate more sophisticated representations of land cover, particularly for areas with high biomass and mixed land cover. In the current modeling, uncertainty is only partly addressed by selecting the goodperforming parameter sets. However, this approach is limited to parameterization uncertainty related to mHM and does not consider either model structural or input data uncertainty. Addressing them requires a more detailed and careful revision of underlying model components (e.g., elaborated soil water or vegetation dynamics) and explicit treatment of different vegetation types (e.g., croplands, grasslands, and extensive pasture areas). This may have particular impact in forested areas with dynamic vegetation components, such as site-specific LAI or rootwater uptake from different layers. Further, a more rigorous uncertainty assessment such as using Bayesian methods or other formal statistical techniques could be used to explicitly quantify and propagate different sources of uncertainties throughout the modeling process. Such an approach should also account for input data uncertainty, particularly that arising from CRNS sensor measurements in complex forest environments (Bogena et al., 2013), as measurement errors and variability in observational data can strongly influence model outcomes.

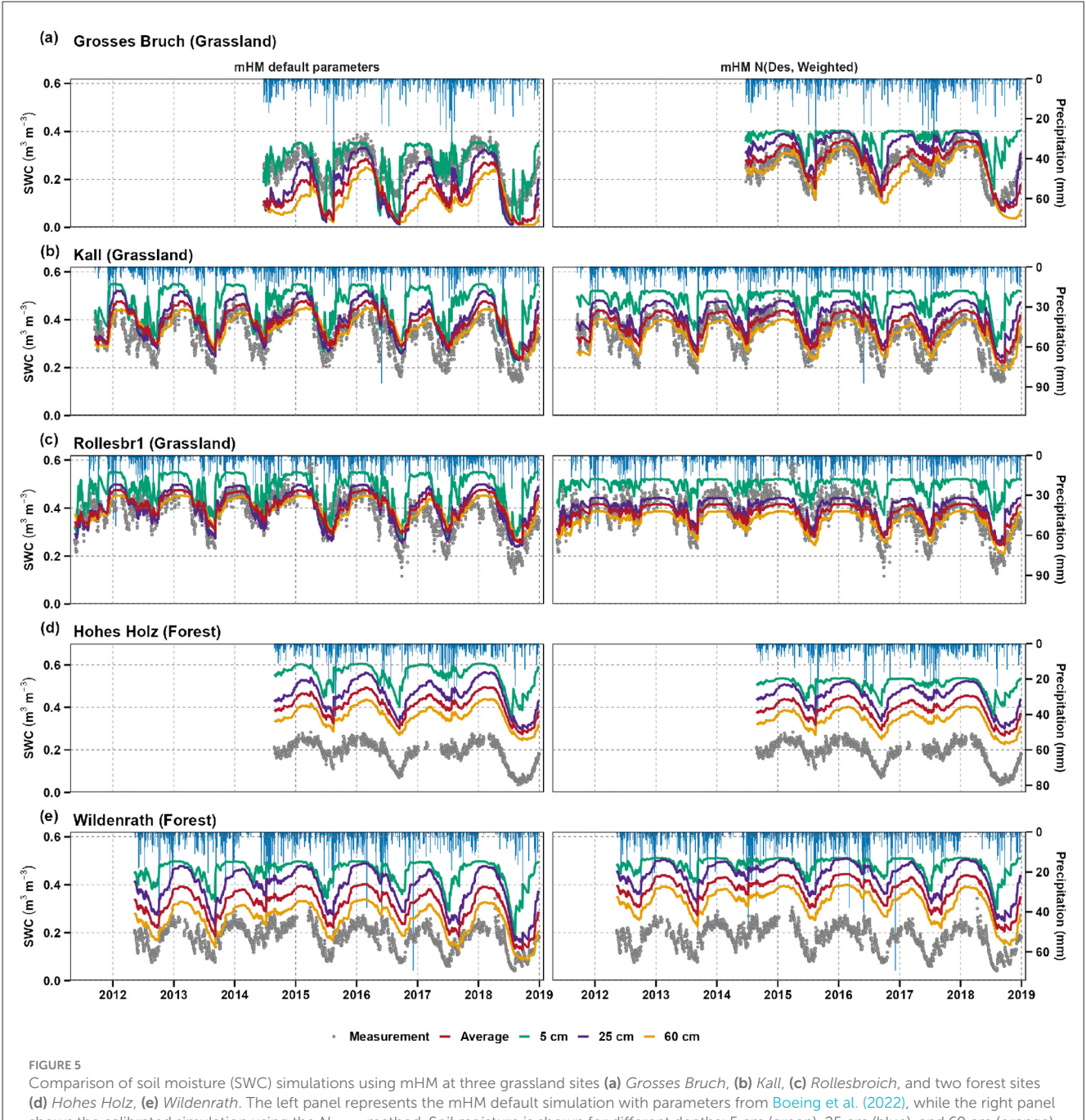
Another promising approach that could potentially enhance the mHM performance is to leverage the recently introduced fast Richards solver, as reported by Kholis et al. (2025). The parameterization of the Richards solver demonstrated strong agreement with point-scale observations, accurately capturing absolute soil water storage (SWS). This could be beneficial for CRNS data assimilation as well.

3.4 Cross-validation of constrained model parametrization

The transferability of calibrated parameters based on CRNS data regionalized for the railway segment between Blankenburg-Rübeland (applied to the Meadow [M] and Forest [F1]), was evaluated for non-calibrated target sites. The soil moisture measurements based on CRNS are available from Bogena et al. (2022). The performance of this parameter transfer is evaluated in Table 2 and Figure 5. The left panels illustrate the default mHM simulation based on the parameters of Boeing et al. (2022), while the right panels show the results of the parameters transferred from the calibration. We selected the 10 sets of optimal parameters with 27 global parameters of snow, soil moisture, and neutron counts as shown in Supplementary Table S1. By doing so, we aimed to assess whether the calibrated model parameters, based on spatio-temporal neutron count data from the rail track, provide adequate information that can be transferred reliably.

At Grosses Bruch, Kall, and Rollesbroich (Figures 5a-c), the parameter transfer significantly improved temporal SWC

10 3389/frwa 2025 1630051 Fatima et al.



shows the calibrated simulation using the $N_{\text{Des W}}$ method. Soil moisture is shown for different depths: 5 cm (green), 25 cm (blue), and 60 cm (orange), along with the average soil moisture (red). Observed CRNS soil moisture measurements are represented by gray dots

dynamics, reflecting the improved NSE (e.g., Grosses Bruch: NSE from -1.51 to 0.5) and reduced PBIAS (e.g., Grosses Bruch: -44.3% to 9.2%) in Table 3. Notably, the parameterized model better captured seasonal soil moisture minima during dry summer periods and reflected quicker recovery after precipitation events. This enhancement is most pronounced in the topsoil (5 cm), consistent with the known sensitivity of CRNS to near-surface moisture variability (Baatz et al., 2014; Rosenbaum et al., 2012). The overall dynamic range and intraannual variability were also more realistically reproduced in the transferred setup.

In Hohes Holz and Wildenrath (Figures 5d, e), there are modest improvements in NSE (e.g., Hohes Holz: -16 to -13.61) but persistently high PBIAS (e.g., 132% to 122.1%), indicating systemic bias. This bias is particularly pronounced at Wildenrath, which exhibits the poorest performance among the sites. The figure's forest panels may reveal persistent mismatches in SWC magnitude, particularly at the upper layer (5 cm), where neutron counts are highly sensitive to the topsoil moisture layers. The deeper soil layers (60 cm) exhibited increased consistency with measured values, particularly during the wetter seasons. Despite higher R² values (e.g., Hohes Holz: 0.82 to 0.84), poor NSE/KGE underscores issues

in magnitude accuracy, which could manifest as phase shifts or amplitude errors in the figure. At *Wildenrath*, SWC did not improve relative to the reference parameters. A potential contributing factor is the difference in land use: unlike the F1 site, which features dense forest cover, the *Wildenrath* site exhibits a less densely vegetated landscape. This divergence in land use characteristics likely accounts for the observed discrepancies in the transferred parameters from the *F1* site. Baatz et al. (2014) reported a very low average soil moisture, but due to the high amount of above-ground biomass at the *Wildenrath* site. Additionally, Bogena et al. (2013) emphasized the uncertainties in CRNS-derived SWC estimates within forested ecosystems, attributing them to various additional hydrogen sources other than soil moisture. These could include above- and below-ground biomass, the litter layer, intercepted canopy water, and soil organic matter.

Across grassland sites, SWC estimates using transferred parameter sets showed improved alignment with CRNS-derived measurements, confirming the utility of integrating neutron count based assimilation approaches in large-scale hydrological modeling. However, in the forest site, we observe a systematic bias, an overestimation of the soil moisture compared to observations. This overestimation may be attributed to the absence of an explicit representation of the litter layer in the mHM under canopy vegetation. Unlike models such as CABLE land surface model (Haverd et al., 2016), which incorporate a physically accurate treatment of the litter layer and its role in mediating soil evaporation and energy fluxes, mHM does not explicitly resolve this component. To improve the model's accuracy, one potential solution would be to incorporate an explicit representation of the litter layer in mHM or explicitly account for litter extraction in the neutron-based measurements (Iwema et al., 2017). This adjustment could reduce the bias and enhance the model's ability to represent the soil moisture dynamics more accurately. Another pragmatic option could also be the introduction of a bias correction factor, which is a typical procedure in climate and hydrological modeling (Su and Ryu, 2015; Fairbairn et al., 2024). The generally significant uncertainty in forested areas indicates a need for further studies to refine model parameterization and processes.

Besides above aspects, another avenue for model improvement lies in the explicit treatment of vegetation dynamics, including phenological development, particularly in forested land cover, as well as the implementation of alternative soil moisture dynamics schemes. Vegetation dynamics, including above-ground biomass, LAI, and their seasonal changes, play a central role in controlling interception, evapotranspiration, and related processes, with strong impacts on root-zone soil moisture. To this end, Bahrami et al. (2022) proposed a parsimonious canopy model (PCM) to predict the daily variability of LAI and other vegetation dynamics (e.g., gross primary productivity, GPP) that are closely linked to root-zone soil moisture processes. Incorporating such a representation, and ongoing efforts to couple PCM with mHM, would enable a more realistic treatment of vegetation-soil interactions in forested regions.

Regarding soil moisture dynamics, in this work mHM currently applies the infiltration-capacity approach, similar to the HBV model (Samaniego et al., 2010b). More recent developments in mHM include an explicit solution of the Richards equation with an improved parameterization approach (Kholis et al.,

2025). Compared to the infiltration-capacity approach, the 1D Richards equation—owing to its two-way flow mechanism—provides improved soil moisture predictions, particularly in deeper soil layers. Ongoing research is investigating how these approaches could translate into better representation of *in-situ* measurements, which remains an active and important task.

The present results collectively demonstrate the potential of rail-based CRNS networks, when coupled with optimal parameter estimation, to support regional-scale soil moisture modeling with limited calibration requirements. However, further analysis is warranted to quantify the spatial limits of transferability, especially across heterogeneous land cover and topographic gradients. These findings support recent developments in hydrological observatories such as TERENO in central Germany (Wollschläger et al., 2017) or TERENO-Rur (Bogena et al., 2018) and strengthen the growing evidence that the use of soil moisture data derived from CRNS or SMAP improves the precision of hydrological models at different scales (Zhao et al., 2025; Li et al., 2024).

4 Conclusions

The availability of mobile cosmic-ray neutron datasets across time and space marks a new era for hydrological model evaluation. Using data from a 9 km railway track passing through different types of land cover in central Germany, we were able for the first time to evaluate the performance of the hydrological model mHM in representing spatial patterns of root-zone soil moisture. By parameter calibration, we achieved significant improvements in model performance, particularly for homogeneous land cover types such as meadows (*M*) and dense forests (*F1*). The calibration improved soil moisture dynamics in the model (e.g., NSE from 0.50 to 0.79 for the meadow) and soil moisture spatial patterns (SPAEF from 0.39 to 0.71 along the whole track). These results underscore the value of CRNS-derived soil moisture data in constraining hydrological model parameters and capturing spatio-temporal dynamics at a 200 m resolution.

These findings demonstrate the potential of a model-data fusion approach, where high-resolution CRNS measurements are integrated into a large-scale hydrological model, to improve regional soil moisture prediction. Furthermore, the transferability of site-calibrated parameters to (other) independent grassland sites validates their robustness for regional applications.

However, challenges persisted at forest sites, where vegetation biomass and the effects of the litter layer may have introduced biases. The systematic overestimation of soil moisture in forests highlighted the need for more sophisticated process descriptions as well as datasets to explicitly represent the dynamics of vegetation and the interactions between soil, plants, and atmosphere in mHM. Better datasets of water dynamics in the litter layer would also help CRNS products to better represent the water content in the soil. It has also been noted that the spatial resolution of mHM is larger than the near-field sensitivity of CRNS measurements, which limits the performance of the spatial pattern comparison especially in mixed landscapes with small-scale heterogeneity. We also emphasize the limitation of spatial transferability of the presented results due to the short length of the investigated rail track. Future extension of the regions covered by CRNS detectors

on rails will provide better coverage of the diversity of land use classes in Germany and, in combination with the multi-scale parameter regionalization of MPR, facilitate better transferability also to ungauged regions.

Overall, the demonstrated value of rail-based CRNS data in hydrological modeling highlights its practical relevance to improve predictions and support sustainable water resource management.

Data availability statement

Publicly available datasets were analyzed in this study. CRNS-Railway data has been used from Altdorff et al. (2023). The terrain elevation data was collected from USGS EROS Archive-Digital Elevation-Global Multi-resolution Terrain Elevation Data 2010 (GMTED2010), available at https://www.usgs.gov/centers/ eros/science/usgs-eros-archive-digital-elevation-global-multiresolution-terrain-elevation. Gridded soil characteristics are based on the BUEK200 database obtained from the German Federal Institute for Geosciences and Natural Resources (BGR, see online https://geoportal.bgr.de/mapapps/resources/apps/geoportal/ index.html?lang=en#/datasets/portal/154997F4-3C14-4A53-B217-8A7C7509E05F). The geological dataset was downloaded from the Institute for Biogeochemistry and Marine Chemistry, KlimaCampus, Universität Hamburg (https://www.geo.unihamburg.de/en/geologie/forschung/aquatische-geochemie/glim. html). Leaf Area Index (LAI) dataset was downloaded from the Global Land Cover Facility (GLCF), available at http://iridl.ldeo. columbia.edu/SOURCES/.UMD/.GLCF/.GIMMS/.NDVIg/.global/ index.html. The land cover dataset was downloaded from the European Space Agency (ESA), available at http://due.esrin.esa.int/ page_globcover.php.

Author contributions

EF: Validation, Data curation, Visualization, Methodology, Formal analysis, Investigation, Software, Writing – original draft, Writing – review & editing. RK: Funding acquisition, Methodology, Writing – review & editing, Supervision, Investigation, Software, Validation, Resources, Conceptualization. DA: Writing – review & editing, Validation, Methodology, Investigation, Data curation. SA: Resources, Project administration, Writing – review & editing, Funding acquisition, Supervision. FB: Visualization, Validation, Conceptualization, Investigation, Writing – review & editing, Methodology. SO: Methodology, Writing – review & editing. OR: Methodology, Data curation, Writing – review & editing. LS: Conceptualization, Writing – review & editing, Methodology. MS: Conceptualization, Investigation, Funding acquisition, Writing – review & editing, Supervision, Methodology.

Funding

The author(s) declare that financial support was received for the research and/or publication of this article. The research was funded by the German Academic Exchange Service (DAAD) through the Graduate School Scholarship Program under Reference

Number 91788160, and additionally supported by the Deutsche Forschungsgemeinschaft (Grant 357874777; research unit FOR 2694, Cosmic Sense II).

Acknowledgments

The authors like to thank the crucial support from the Havelländische Eisenbahn Gesellschaft (HVLE), Wustermark, Germany, particularly from Dirk Brandenburg and Uwe Wullstein. The study has been made possible by the Terrestrial Environmental Observatories (TERENO), an infrastructural fund of the Helmholtz Association. We particularly thank Corinna Rebmann and Heye Bogena for sharing the datasets of the TERENO sites Hohes Holz, Großes Bruch, Kall, Wildenrath, and Rollesbroich. The high-performance computing cluster EVE has contributed to the computation of the scientific findings. Eshrat Fatima is grateful for the financial support of the German Academic Exchange Service (DAAD) through the Graduate School Scholarship Program under Reference Number 91788160. We kindly acknowledge the German Weather Service (DWD) for providing the meteorological datasets.

Conflict of interest

The authors declare that the research was conducted in the absence of any commercial or financial relationships that could be construed as a potential conflict of interest.

The author(s) declared that they were an editorial board member of Frontiers, at the time of submission. This had no impact on the peer review process and the final decision.

The handling editor LB declared a past co-authorship with the authors SA and LS.

Generative AI statement

The author(s) declare that no Gen AI was used in the creation of this manuscript.

Any alternative text (alt text) provided alongside figures in this article has been generated by Frontiers with the support of artificial intelligence and reasonable efforts have been made to ensure accuracy, including review by the authors wherever possible. If you identify any issues, please contact us.

Publisher's note

All claims expressed in this article are solely those of the authors and do not necessarily represent those of their affiliated organizations, or those of the publisher, the editors and the reviewers. Any product that may be evaluated in this article, or claim that may be made by its manufacturer, is not guaranteed or endorsed by the publisher.

Supplementary material

The Supplementary Material for this article can be found online at: https://www.frontiersin.org/articles/10.3389/frwa.2025. 1630051/full#supplementary-material

References

- Altdorff, D., Oswald, S. E., Zacharias, S., Zengerle, C., Dietrich, P., Mollenhauer, H., et al. (2023). Toward large-scale soil moisture monitoring using rail-based cosmic ray neutron sensing. *Water Resour. Res.* 59:e2022WR033514. doi: 10.1029/2022WR03514
- Andreasen, M., Jensen, K. H., Desilets, D., Franz, T. E., Zreda, M., Bogena, H. R., et al. (2017). Status and perspectives on the cosmic-ray neutron method for soil moisture estimation and other environmental science applications. *Vadose Zone J.* 16, 1–11. doi: 10.2136/vzj2017.04.0086
- Arnault, J., Fersch, B., Schrön, M., Bogena, H. R., Hendricks Franssen, H.-J., and Kunstmann, H. (2025). Role of infiltration on land-atmosphere feedbacks in central Europe: fully coupled wrf-hydro simulations evaluated with cosmic-ray neutron soil moisture measurements. *J. Hydrometeorol.* 26, 129–153. doi: 10.1175/JHM-D-24-0049.1
- Avery, W. A., Finkenbiner, C., Franz, T. E., Wang, T., Nguy-Robertson, A. L., Suyker, A., et al. (2016). Incorporation of globally available datasets into the roving cosmic-ray neutron probe method for estimating field-scale soil water content. *Hydrol. Earth Syst. Sci.* 20, 3859–3872. doi: 10.5194/hess-20-3859-2016
- Baatz, R., Bogena, H., Franssen, H.-J. H., Huisman, J., Qu, W., Montzka, C., et al. (2014). Calibration of a catchment scale cosmic-ray probe network: a comparison of three parameterization methods. *J. Hydrol.* 516, 231–244. doi: 10.1016/j.jhydrol.2014.02.026
- Baatz, R., Bogena, H., Hendricks Franssen, H.-J., Huisman, J., Montzka, C., and Vereecken, H. (2015). An empirical vegetation correction for soil water content quantification using cosmic ray probes. *Water Resour. Res.* 51, 2030–2046. doi: 10.1002/2014WR016443
- Baatz, R., Hendricks Franssen, H.-J., Han, X., Hoar, T., Bogena, H. R., and Vereecken, H. (2017). Evaluation of a cosmic-ray neutron sensor network for improved land surface model prediction. *Hydrol. Earth Syst. Sci.* 21, 2509–2530. doi:10.5194/hess-21-2509-2017
- Bahrami, B., Hildebrandt, A., Thober, S., Rebmann, C., Fischer, R., Samaniego, L., et al. (2022). Developing a parsimonious canopy model (pcm v1. 0) to predict forest gross primary productivity and leaf area index of deciduous broad-leaved forest. *Geosci. Model Dev.* 15, 6957–6984. doi: 10.5194/gmd-15-6957-2022
- BGR. (2020). Digital soil map of Germany (BUEK 200) v0.5. Federal Institute for Geosciences and Natural Resources, Hannover. Available online at: https://www.bgr.bund.de/DE/Themen/Boden/Projekte/Flaechen_Rauminformationen_Boden/BUEK200/BUEK200.html?nn=869002(Accessed September 2025).
- Boeing, F., Rakovec, O., Kumar, R., Samaniego, L., Schrön, M., Hildebrandt, A., et al. (2022). High-resolution drought simulations and comparison to soil moisture observations in Germany. *Hydrol. Earth Syst. Sci.* 26, 5137–5161. doi: 10.5194/hess-26-5137-2022
- Bogena, H., Huisman, J., Baatz, R., Hendricks Franssen, H.-J., and Vereecken, H. (2013). Accuracy of the cosmic-ray soil water content probe in humid forest ecosystems: the worst case scenario. *Water Resour. Res.* 49, 5778–5791. doi:10.1002/wrcr.20463
- Bogena, H., Montzka, C., Huisman, J., Graf, A., Schmidt, M., Stockinger, M., et al. (2018). The tereno-rur hydrological observatory: a multiscale multi-compartment research platform for the advancement of hydrological science. *Vadose Zone J.* 17, 1–22. doi: 10.2136/vzj2018.03.0055
- Bogena, H. R., Schrön, M., Jakobi, J., Ney, P., Zacharias, S., Andreasen, M., et al. (2022). Cosmos-europe: a European network of cosmic-ray neutron soil moisture sensors. *Earth Syst. Sci. Data* 14, 1125–1151. doi: 10.5194/essd-14-1125-2022
- Corradini, C. (2014). Soil moisture in the development of hydrological processes and its determination at different spatial scales. *J. Hydrol.* 516, 1–5. doi: 10.1016/j.jhydrol.2014.02.051
- Demirci, U., and Demirel, M. C. (2023). Effect of dynamic pet scaling with lai and aspect on the spatial performance of a distributed hydrologic model. *Agronomy* 13:534. doi: 10.3390/agronomy13020534
- Demirel, M. C. (2020). SPAEF Version 2.0 (Auto-Detected Number of Bins) (v2.0). Zenodo. doi: 10.5281/zenodo.5861253
- Demirel, M. C., Mai, J., Mendiguren, G., Koch, J., Samaniego, L., and Stisen, S. (2018). Combining satellite data and appropriate objective functions for improved spatial pattern performance of a distributed hydrologic model. *Hydrol. Earth Syst. Sci.* 22, 1299–1315. doi: 10.5194/hess-22-1299-2018
- Duethmann, D., Anderson, M., Maneta, M. P., and Tetzlaff, D. (2024). Improving process-consistency of an ecohydrological model through inclusion of spatial patterns of satellite-derived land surface temperature. *J. Hydrol.* 628:130433. doi: 10.1016/j.jhydrol.2023.130433
- Duygu, M. B., and Akyürek, Z. (2019). Using cosmic-ray neutron probes in validating satellite soil moisture products and land surface models. *Water* 11:1362. doi: 10.3390/w11071362

- Eini, M. R., Massari, C., and Piniewski, M. (2023). Satellite-based soil moisture enhances the reliability of agro-hydrological modeling in large transboundary river basins. *Sci. Total Environ.* 873:162396. doi: 10.1016/j.scitotenv.2023.162396
- Entekhabi, D., Yueh, S. I., and Lannoy, G. D. (2014). SMAP Handbook-soil Moisture Active Passive: Mapping Soil Moisture and Freeze/thaw From Space. Technical report, NASA Jet Propulsion Laboratory.
- ESA and UCLouvain (2010). GlobCover 2009 Global Land Cover Map. European Space Agency and Université Catholique de Louvain.
- Fairbairn, D., De Rosnay, P., and Weston, P. (2024). Evaluation of an adaptive soil moisture bias correction approach in the ecmwf land data assimilation system. *Remote Sens.* 16:493. doi: 10.3390/rs16030493
- Fang, B., Lakshmi, V., and Zhang, R. (2024). Validation of downscaled 1-km smos and smap soil moisture data in 2010–2021. *Vadose Zone J.* 23:e20305. doi: 10.1002/vzi2.20305
- Fatichi, S., Vivoni, E. R., Ogden, F. L., Ivanov, V. Y., Mirus, B., Gochis, D., et al. (2016). An overview of current applications, challenges, and future trends in distributed process-based models in hydrology. *J. Hydrol.* 537, 45–60. doi: 10.1016/j.jhydrol.2016.03.026
- Fatima, E., Kumar, R., Attinger, S., Kaluza, M., Rakovec, O., Rebmann, C., et al. (2024). Improved representation of soil moisture processes through incorporation of cosmic-ray neutron count measurements in a large-scale hydrologic model. *Hydrol. Earth Syst. Sci.* 28, 5419–5441. doi: 10.5194/hess-28-5419-2024
- Gnann, S., Reinecke, R., Stein, L., Wada, Y., Thiery, W., Müller Schmied, H., et al. (2023). Functional relationships reveal differences in the water cycle representation of global water models. *Nat. Water* 1, 1079–1090. doi: 10.1038/s44221-023-00160-y
- Greacen, E. L. (1981). Soil water assessment by the neutron method. CSIRO. (Accessed June 1, 2021).
- Gupta, H. V., Kling, H., Yilmaz, K. K., and Martinez, G. F. (2009). Decomposition of the mean squared error and nse performance criteria: Implications for improving hydrological modelling. *J. Hydrol.* 377, 80–91. doi: 10.1016/j.jhydrol.2009.08.003
- Han, X., Franssen, H.-J., Rosolem, R., Jin, R., Li, X., and Vereecken, H. (2015). Correction of systematic model forcing bias of clm using assimilation of cosmic-ray neutrons and land surface temperature: a study in the heihe catchment, China. *Hydrol. Earth Syst. Sci.* 19, 615–629. doi: 10.5194/hess-19-615-2015
- Hartmann, J., and Moosdorf, N. (2012). The new global lithological map database glim: a representation of rock properties at the earth surface. *Geochem. Geophys. Geosyst.* 13. doi: 10.1029/2012GC004370
- Haverd, V., Cuntz, M., Nieradzik, L. P., and Harman, I. N. (2016). Improved representations of coupled soil-canopy processes in the cable land surface model (subversion revision 3432). *Geosci. Model Dev.* 9, 3111–3122. doi: 10.5194/gmd-9-3111-2016
- Iwema, J., Rosolem, R., Rahman, M., Blyth, E., and Wagener, T. (2017). Land surface model performance using cosmic-ray and point-scale soil moisture measurements for calibration. *Hydrol. Earth Syst. Sci.* 21, 2843–2861. doi: 10.5194/hess-21-2843-2017
- Kaspar, F., Müller-Westermeier, G., Penda, E., Mächel, H., Zimmermann, K., Kaiser-Weiss, A., et al. (2013). Monitoring of climate change in Germany data, products and services of Germany's National Climate Data Centre. *Adv. Sci. Res.* 10, 99–106. doi: 10.5194/asr-10-99-2013
- Kholis, A., Kalbacher, T., Rakovec, O., Boeing, F., Cuntz, M., and Samaniego, L. (2025). Evaluating richards equation and infiltration capacity approaches in mesoscale hydrologic modeling. *Water Resour. Res.* 61:e2024WR039625. doi: 10.1029/2024WR039625
- Koch, J., Demirel, M. C., and Stisen, S. (2018). The spatial efficiency metric (SPAEF): multiple-component evaluation of spatial patterns for optimization of hydrological models. *Geosci. Model Dev.* 11, 1873–1886. doi: 10.5194/gmd-11-1873-2018
- Köhli, M., Schrön, M., Zreda, M., Schmidt, U., Dietrich, P., and Zacharias, S. (2015). Footprint characteristics revised for field-scale soil moisture monitoring with cosmic-ray neutrons. *Water Resour. Res.* 51, 5772–5790. doi: 10.1002/2015WR017169
- Köhli, M., Weimar, J., Schrön, M., Baatz, R., and Schmidt, U. (2021). Soil moisture and air humidity dependence of the above-ground cosmic-ray neutron intensity. *Front. Water* 2:544847. doi: 10.3389/frwa.2020.544847
- Kumar, R., Livneh, B., and Samaniego, L. (2013a). Toward computationally efficient large-scale hydrologic predictions with a multiscale regionalization scheme. *Water Resour. Res.* 49, 5700–5714. doi: 10.1002/wrcr.20431
- Kumar, R., Samaniego, L., and Attinger, S. (2013b). Implications of distributed hydrologic model parameterization on water fluxes at multiple scales and locations. *Water Resour. Res.* 49, 360–379. doi: 10.1029/2012WR012195
- Li, F., Bogena, H. R., Bayat, B., Kurtz, W., and Hendricks Franssen, H.-J. (2024). Can a sparse network of cosmic ray neutron sensors improve soil moisture and evapotranspiration estimation at the larger catchment scale? *Water Resour. Res.* 60:e2023WR035056. doi: 10.1029/2023WR035056

- Marx, A., Kumar, R., Thober, S., Rakovec, O., Wanders, N., Zink, M., et al. (2018). Climate change alters low flows in europe under global warming of 1.5, 2, and 3 c. *Hydrol. Earth Syst. Sci.* 22, 1017–1032. doi: 10.5194/hess-22-1017-2018
- Massoud, E. C., Xu, C., Fisher, R. A., Knox, R. G., Walker, A. P., Serbin, S. P., et al. (2019). Identification of key parameters controlling demographically structured vegetation dynamics in a land surface model: CLM4. 5 (fates). *Geosci. Model Dev.* 12, 4133–4164. doi: 10.5194/gmd-12-4133-2019
- McKay, M., and Conover, W. (1979). Rj beckman a comparison of three methods for selecting values of input variables in the analysis of output from a computer code. *Technometrics* 21, 239–245. doi: 10.1080/00401706.1979.10489755
- Moges, E., Demissie, Y., Larsen, L., and Yassin, F. (2020). Review: sources of hydrological model uncertainties and advances in their analysis. *Water* 13:28. doi: 10.3390/w13010028
- Moriasi, D. N., Arnold, J. G., Van Liew, M. W., Bingner, R. L., Harmel, R. D., and Veith, T. L. (2007). Model evaluation guidelines for systematic quantification of accuracy in watershed simulations. *Trans. ASABE* 50, 885–900. doi: 10.13031/2013.23153
- Nash, J. E., and Sutcliffe, J. V. (1970). River flow forecasting through conceptual models part i—a discussion of principles. *J. Hydrol.* 10, 282–290. doi:10.1016/0022-1694(70)90255-6
- Nguyen, T. V., Uniyal, B., Tran, D. A., and Pham, T. B. T. (2022). On the evaluation of both spatial and temporal performance of distributed hydrological models using remote sensing products. *Remote Sens.* 14:1959. doi: 10.3390/rs14091959
- Oswald, S. E., Angermann, L., Bogena, H. R., Förster, M., García-García, A., Lischeid, G., et al. (2024). Hydrology on solid grounds? Integration is key to closing knowledge gaps concerning landscape subsurface water storage dynamics. *Hydrol. Process.* 38:e15320. doi: 10.1002/hyp.15320
- Patil, A., Fersch, B., Hendricks Franssen, H.-J., and Kunstmann, H. (2021). Assimilation of cosmogenic neutron counts for improved soil moisture prediction in a distributed land surface model. *Front. Water* 3:729592. doi: 10.3389/frwa.2021.729592
- Rakovec, O., Kumar, R., Mai, J., Cuntz, M., Thober, S., Zink, M., et al. (2016). Multiscale and multivariate evaluation of water fluxes and states over european river basins. *J. Hydrometeorol.* 17, 287–307. doi: 10.1175/JHM-D-15-0054.1
- Renard, B., Kavetski, D., Kuczera, G., Thyer, M., and Franks, S. W. (2010). Understanding predictive uncertainty in hydrologic modeling: the challenge of identifying input and structural errors. *Water Resour. Res.* 46:WR008328. doi:10.1029/2009WR008328
- Rosenbaum, U., Bogena, H. R., Herbst, M., Huisman, J. A., Peterson, T. J., Weuthen, A., et al. (2012). Seasonal and event dynamics of spatial soil moisture patterns at the small catchment scale. *Water Resour. Res.* 48:WR011518. doi: 10.1029/2011WR011518
- Samaniego, L. (2025). Permanent shifts in the global water cycle. *Science* 387, 1348–1350. doi: 10.1126/science.adw5851
- Samaniego, L., Bárdossy, A., and Kumar, R. (2010a). Streamflow prediction in ungauged catchments using copula-based dissimilarity measures. *Water Resour. Res.* 46:WR007695. doi: 10.1029/2008WR007695
- Samaniego, L., Kumar, R., and Attinger, S. (2010b). Multiscale parameter regionalization of a grid-based hydrologic model at the mesoscale. *Water Resour. Res.* 46:WR007327. doi: 10.1029/2008WR007327
- Samaniego, L., Kumar, R., Thober, S., Rakovec, O., Zink, M., Wanders, N., et al. (2017). Toward seamless hydrologic predictions across spatial scales. *Hydrol. Earth Syst. Sci.* 21, 4323–4346. doi: 10.5194/hess-21-4323-2017
- Samaniego, L., Kumar, R., and Zink, M. (2013). Implications of parameter uncertainty on soil moisture drought analysis in Germany. *J. Hydrometeorol.* 14, 47–68. doi: 10.1175/JHM-D-12-075.1
- Scheiffele, L. M., Munz, M., Francke, T., Baroni, G., and Oswald, S. E. (2025). Enhancing hectare-scale groundwater recharge estimation by integrating data from cosmic-ray neutron sensing into soil hydrological modeling. *Water Resour. Res.* 61:e2024WR037641. doi: 10.1029/2024WR037641
- Schrön, M., Köhli, M., Scheiffele, L., Iwema, J., Bogena, H. R., Lv, L., et al. (2017). Improving calibration and validation of cosmic-ray neutron sensors in the light of spatial sensitivity. *Hydrol. Earth Syst. Sci.* 21, 5009–5030. doi:10.5194/hess-21-5009-2017
- Schrön, M., Köhli, M., and Zacharias, S. (2023). Signal contribution of distant areas to cosmic-ray neutron sensors–implications for footprint and sensitivity. *Hydrol. Earth Syst. Sci.* 27, 723–738. doi: 10.5194/hess-27-723-2023

- Schrön, M., Oswald, S. E., Zacharias, S., Kasner, M., Dietrich, P., and Attinger, S. (2021). Neutrons on rails: transregional monitoring of soil moisture and snow water equivalent. *Geophys. Res. Lett.* 48:e2021GL093924. doi: 10.1029/2021GL093924
- Schrön, M., Rosolem, R., Köhli, M., Piussi, L., Schröter, I., Iwema, J., et al. (2018a). Cosmic-ray neutron rover surveys of field soil moisture and the influence of roads. *Water Resour. Res.* 54, 6441–6459. doi: 10.1029/2017WR02 1719
- Schrön, M., Zacharias, S., Womack, G., Köhli, M., Desilets, D., Oswald, S. E., et al. (2018b). Intercomparison of cosmic-ray neutron sensors and water balance monitoring in an urban environment. *Geosci. Instrum. Methods Data Syst.* 7, 83–99. doi: 10.5194/gi-7-83-2018
- Seneviratne, S. I., Corti, T., Davin, E. L., Hirschi, M., Jaeger, E. B., Lehner, I., et al. (2010). Investigating soil moisture-climate interactions in a changing climate: a review. *Earth-Sci. Rev.* 99, 125–161. doi: 10.1016/j.earscirev.2010.02.004
- Shepard, D. (1968). "A two-dimensional interpolation function for irregularly-spaced data," in *Proceedings of the 1968 23rd ACM National Conference*, 517–524. doi: 10.1145/800186.810616
- Soltani, M., Bjerre, E., Koch, J., and Stisen, S. (2021). Integrating remote sensing data in optimization of a national water resources model to improve the spatial pattern performance of evapotranspiration. *J. Hydrol.* 603:127026. doi:10.1016/j.jhydrol.2021.127026
- Su, C.-H., and Ryu, D. (2015). Multi-scale analysis of bias correction of soil moisture. *Hydrol. Earth Syst. Sci.* 19, 17–31. doi: 10.5194/hess-19-17-2015
- Teweldebrhan, A. T., Burkhart, J. F., and Schuler, T. V. (2018). Parameter uncertainty analysis for an operational hydrological model using residual-based and limits of acceptability approaches. *Hydrol. Earth Syst. Sci.* 22, 5021–5039. doi: 10.5194/hess-22-5021-2018
- Thober, S., Kumar, R., Sheffield, J., Mai, J., Schäfer, D., and Samaniego, L. (2015). Seasonal soil moisture drought prediction over europe using the North American multi-model ensemble (NMME). *J. Hydrometeorol.* 16, 2329–2344. doi: 10.1175/JHM-D-15-0053.1
- Tiwari, D., Trudel, M., and Leconte, R. (2023). On optimization of calibrations of a distributed hydrological model with spatially distributed information on snow. *Hydrol. Earth Syst. Sci. Discuss.* 2023, 1–28. doi: 10.5194/hess-2023-143
- USGS. (2017). Global Multi-resolution Terrain Elevation Data 2010 (GMTED2010). Type: dataset.
- Winter, C., Lutz, S. R., Musolff, A., Kumar, R., Weber, M., and Fleckenstein, J. H. (2021). Disentangling the impact of catchment heterogeneity on nitrate export dynamics from event to long-term time scales. *Water Resour. Res.* 57:e2020WR027992. doi: 10.1029/2020WR027992
- Wollschläger, U., Attinger, S., Borchardt, D., Brauns, M., Cuntz, M., Dietrich, P., et al. (2017). The bode hydrological observatory: a platform for integrated, interdisciplinary hydro-ecological research within the tereno harz/central german lowland observatory. *Environ. Earth Sci.* 76, 1–25. doi: 10.1007/s12665-016-63
- Yang, X., Jomaa, S., Zink, M., Fleckenstein, J. H., Borchardt, D., and Rode, M. (2018). A new fully distributed model of nitrate transport and removal at catchment scale. *Water Resour. Res.* 54, 5856–5877. doi: 10.1029/2017WR022380
- Zacharias, S., and Wessolek, G. (2007). Excluding organic matter content from pedotransfer predictors of soil water retention. *Soil Sci. Soc. Am. J.* 71, 43–50. doi: 10.2136/sssaj2006.0098
- Zhao, H., Montzka, C., Keller, J., Li, F., Vereecken, H., and Franssen, H.-J. H. (2025). How does assimilating smap soil moisture improve characterization of the terrestrial water cycle in an integrated land surface-subsurface model? *Water Resour. Res.* 61:e2024WR038647. doi: 10.1029/2024WR038647
- Zheng, Y., Coxon, G., Woods, R., Power, D., Rico-Ramirez, M. A., McJannet, D., et al. (2024). Evaluation of reanalysis soil moisture products using cosmic ray neutron sensor observations across the globe. *Hydrol. Earth Syst. Sci.* 28, 1999–2022. doi: 10.5194/hess-28-1999-2024
- Zink, M., Kumar, R., Cuntz, M., and Samaniego, L. (2017). A high-resolution dataset of water fluxes and states for germany accounting for parametric uncertainty. *Hydrol. Earth Syst. Sci.* 21, 1769–1790. doi: 10.5194/hess-21-1769-2017
- Zreda, M., Desilets, D., Ferré, T., and Scott, R. L. (2008). Measuring soil moisture content non-invasively at intermediate spatial scale using cosmic-ray neutrons. *Geophys. Res. Lett.* 35:L21402. doi: 10.1029/2008GL035655